Synthesis of visible and near-infrared light responsed $Sn_{1-x}Bi_xS_2$ for efficient degradation of high concentration rhodamine B

Hui Li[1], Xiang-Feng Wu[1] ✉, Mai-Tuo Yu[1], Yi-Jin Wang[1], Chen-Xu Zhang[1], Jun-Zhang Su[1], Jia-Rui Zhang[1], Ying Zhang[1], Jun-Cheng Pan[1], Chao Wang[1], Yan-Mei Feng[1,2]

[1]*School of Materials Science and Engineering, Hebei Provincial Key Laboratory of Traffic Engineering Materials, Shijiazhuang Tiedao University, Shijiazhuang 050043, People's Republic of China*
[2]*School of Science, North University of China, Taiyuan 030051, People's Republic of China*
✉ *E-mail: wuxiangfeng@stdu.edu.cn*

Published in Micro & Nano Letters; Received on 9th October 2017; Revised on 28th November 2017; Accepted on 7th December 2017

Visible and near-infrared light responsed $Sn_{1-x}Bi_xS_2$nanosheets was synthesised via a simple hydrothermal method. Rhodamine B was adopted to evaluate the degradation efficiency of the as-prepared samples. Experimental results showed that the doping content of Bi^{3+} could obviously affect the degradation efficiency of SnS_2. It was first increased and then decreased with increasing the Bi^{3+} content under the visible light irradiation. When the mole fraction of doping Bi^{3+} was 5%, the as-prepared $Sn_{0.95}Bi_{0.05}S_2$ with a bandgap of 0.38 eV had the highest degradation efficiency of 95.9% in 120 min. Moreover, the as-prepared composites possessed more effective electron–hole pair separation than that of pure SnS_2. In addition, a possible degradation mechanism of the as-prepared $Sn_{0.95}Bi_{0.05}S_2$ was proposed.

1. Introduction: Recently, water pollution has become an emergent problem worldwide. Semiconductor photocatalysts have gained much attention due to their potential applications in solving water pollution [1, 2]. However, the traditional semiconductors, such as TiO_2 [3] and CuO [4], are limited by their wide bandgap energy (>3.2 eV), only sensitive to ultraviolet light, unable to make good use of the sunlight. Recently, much research has been devoted to the exploration of metal sulphides, such as Bi_2S_3 [5], $ZnIn_2S_4$ [6], SnS_2 [7], as their bandgap energy is lower than 2.9 eV. Among these photocatalysts, SnS_2 possesses great potential because of its low cost, low toxicity, wide range of response in visible and near-infrared regions. However, the limited photocatalytic activity restrains its further development and application. Doping metal ions, such as Bi^{3+}, has been proven to be an effective method to enhance the light absorption and photocatalytic properties of semiconductors [8, 9].

In this work, $Sn_{1-x}Bi_xS_2$ was synthesised via a hydrothermal process. Experimental results showed that doping Bi^{3+} could improve the degradation efficiency of pure SnS_2 for rhodamine B (RhB) solution. It might provide reference values for visible and near-infrared light responsed photocatalysis.

2. Experimental section: In a typical procedure, 10 mmol $SnCl_4{\cdot}5H_2O$ (3.5 g) and 66.6 mmol thioacetamide (5.0 g) were dissolved in 70 ml deionised water. Then, a certain amount of Bi $(NO_3)_3{\cdot}5H_2O$ [0.1, 0.3, 0.5 and 0.7 mmol, and the molar ratio of $Bi(NO_3)_3{\cdot}5H_2O$ to $SnCl_4{\cdot}5H_2O$ was 0.01, 0.03, 0.05 and 0.07] was added into the above solution and ultrasonicated for 0.5 h to form suspension. Subsequently, the obtained suspension was transferred into a 100 ml Teflon-lined autoclave and heated at 180°C for 10 h. Finally, the samples were cooled to room temperature, washed with deionised water and ethanol for several times, and dried in an drum wind drying oven at 60°C for 8 h before their further characterisations. The as-prepared samples were defined as $Sn_{1-x}Bi_xS_2$ ($x = 0.01$, 0.03, 0.05 and 0.07, respectively). For comparison, pure SnS_2 was prepared via the same method without using any $Bi(NO_3)_3{\cdot}5H_2O$.

The photocatalytic activity of the as-prepared samples was evaluated by degradation of RhB. A 300 W Xe lamp was used as the light source equipped with a cutoff filter ($\lambda > 420$ nm). In a typical measurement, 50 mg photocatalyst was mixed with 150 ml high concentration (40 mg l^{-1}) of RhB solution. Before the illumination, the suspension solution was stirred in the dark for 1 h to reach the equilibrium of absorption–desorption. The absorbance of RhB solution was measured by a visible spectrophotometer.

3. Results and discussion: Fig. 1*a* shows XRD patterns of pure SnS_2 and the as-synthesised $Sn_{1-x}Bi_xS_2$ with doping various contents of Bi^{3+}. It can be seen that the diffraction peaks of pure SnS_2 were at $2\theta = 15.05°$, 28.30°, 32.21°, 50.11° and 52.62°, indexed to (001), (100), (011), (110), (111) according to PDF# 83-1705. No obvious peaks of any other phases or impurities, such as Bi_2S_3, were observed after doping Bi^{3+}. This result indicated that the as-prepared $Sn_{1-x}Bi_xS_2$possessed a single phase and high purity. Moreover, it can be seen that the width of all the diffraction peaks was broadened with increasing the content of Bi^{3+}. This was caused by the decreased crystallinity. It might be that more and more Sn^{4+} were replaced by Bi^{3+} with increasing the Bi^{3+} content, and a large number of defects were introduced into the lattice. Moreover, the lattice distortion and strain were significantly intensified, might disturb the crystallisation and cause to a decreased crystallinity. In Fig. 1*b*, the magnified view of (001) crystallographic planes are displayed, which show the peaks tend to shift to lower 2θ angles [15.05° for pure SnS_2 and 15.04, 15.03, 15.01, 14.95° for the as-prepared $Sn_{1-x}Bi_xS_2$ ($x = 0.01$, 0.03, 0.05 and 0.07)] with increasing the doping Bi^{3+} content. These results illustrated that Sn^{4+} were successfully replaced by Bi^{3+}. The schematic diagram was shown in Fig. 2.

Fig. 3*a* shows UV–Vis diffuse reflectance spectroscopy (DRS) of pure SnS_2 and the as-synthesised $Sn_{1-x}Bi_xS_2$ with doping various contents of Bi^{3+} from 300 to 1000 nm. It can be seen that all samples possessed obvious absorption in the visible and near-infrared range. Moreover, all the as-prepared $Sn_{1-x}Bi_xS_2$ with doping various Bi^{3+} contents exhibited an enhanced light absorption compared with that of pure SnS_2. The similar phenomenon could also been found in $Sn_{1-x}Ag_xS_2$ with doping various Ag^+ contents [10]. This was in favour of the degradation of RhB solution. As shown in Fig. 3*b*, it can be observed that all the as-prepared $Sn_{1-x}Bi_xS_2$ with doping various contents of Bi^{3+} showed smaller

© The Institution of Engineering and Technology 2017

bandgap energy than that of pure SnS_2. When the mole fraction of doping Bi^{3+} was 5%, the bandgap energy reached the minimum value of 0.38 eV. This was much narrower than 1.58 eV of pure SnS_2, indicating that slight Bi^{3+} could effectively narrow the bandgap of pure SnS_2.

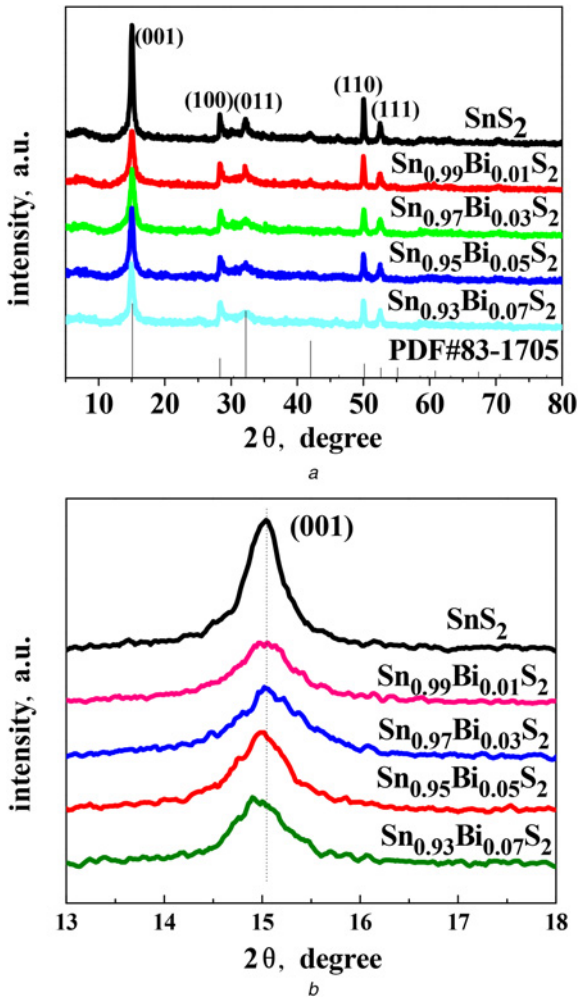

Fig. 1 *XRD patterns and (001) peaks of pure SnS_2 and the as-prepared $Sn_{1-x}Bi_xS_2$*
a XRD patterns of pure SnS_2 and the as-prepared $Sn_{1-x}Bi_xS_2$ with doping various contents of Bi^{3+}
b (001) peaks of pure SnS_2 and the as-prepared $Sn_{1-x}Bi_xS_2$ with doping various contents of Bi^{3+}

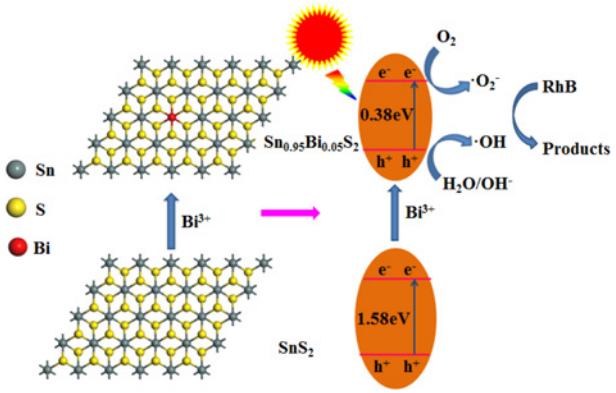

Fig. 2 *Possible degradation mechanism of the as-prepared $Sn_{0.95}Bi_{0.05}S_2$ nanosheets*

The degradation efficiency of the as-prepared samples was evaluated by degradation of high concentration (40 mg l^{-1}) of RhB under the visible-light irradiation. As is shown in Fig. 4*a*, it can be seen the adsorption capacity gradually increased with increasing the doping content of Bi^{3+}. Moreover, doping Bi^{3+} could improve the degradation efficiency of pure SnS_2. The overall degradation efficiency of the as-prepared $Sn_{1-x}Bi_xS_2$ was increased and then decreased with increasing the doping content. When the mole fraction of doping Bi^{3+} was 5%, the as-prepared $Sn_{0.95}Bi_{0.05}S_2$ had the highest degradation efficiency of 95.9% in 120 min. In Fig. 4*b*, the photocatalytic efficiency of the as-prepared samples under the visible light irradiation is shown. Similar results were obtained as in Fig. 4*a*. When the mole fraction of doping Bi^{3+} was 5%, it exhibited the highest photocatalytic efficiency of 80.27% in 120 min. However, when the mole fraction of doping Bi^{3+} increased to 7%, it was not further increased. This might be because that lattice disorder was enhanced with increasing the doping Bi^{3+} content. Excessive Bi^{3+} could not enter the lattice or further narrow the bandgap.

In Fig. 5, it shows the elements composition and chemical states of the as-prepared $Sn_{0.95}Bi_{0.05}S_2$. Fig. 5*a* revealed only Sn, S and Bi peaks existed in the survey spectra of the as-prepared $Sn_{0.95}Bi_{0.05}S_2$, besides C and O from surface contamination. It illustrated that high purity of the as-prepares sample was obtained. As is shown in Fig. 5*b*, there were two peaks of Sn 3d located at 486.9 and 495.3 eV, which were attributed to the Sn $3d_{5/2}$ and Sn $3d_{3/2}$

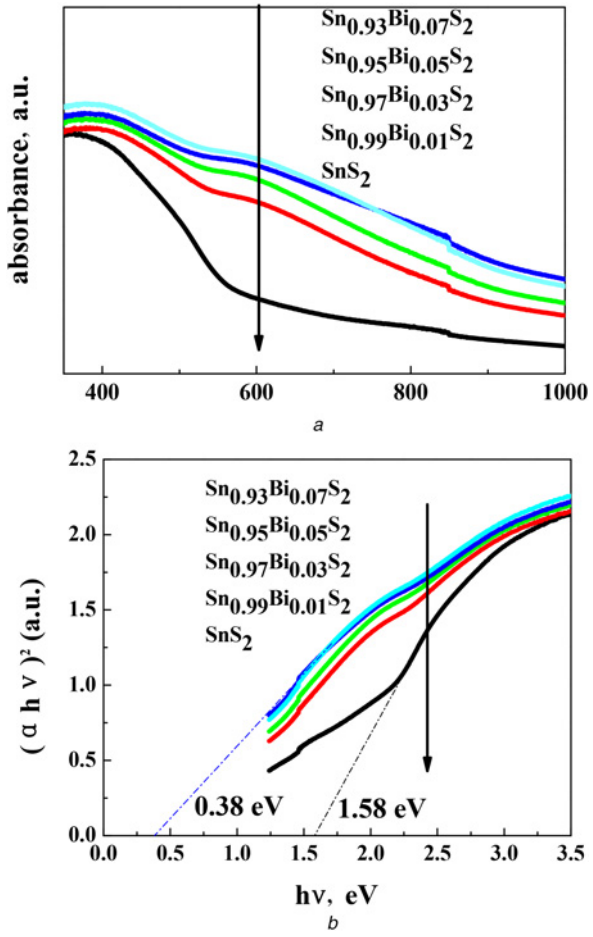

Fig. 3 *UV–Vis DRS and calculation of the bandgap energy of pure SnS_2 and the as-prepared $Sn_{1-x}Bi_xS_2$*
a UV–Vis DRS of pure SnS_2 and the as-prepared $Sn_{1-x}Bi_xS_2$ with doping various contents of Bi^{3+}
b Calculation of the bandgap energy of pure SnS_2 and the as-prepared $Sn_{1-x}Bi_xS_2$ with doping various contents of Bi^{3+} based on the $(\alpha h\nu)^2$–$h\nu$ curve

© The Institution of Engineering and Technology 2017

doi: 10.1049/mnl.2017.0727

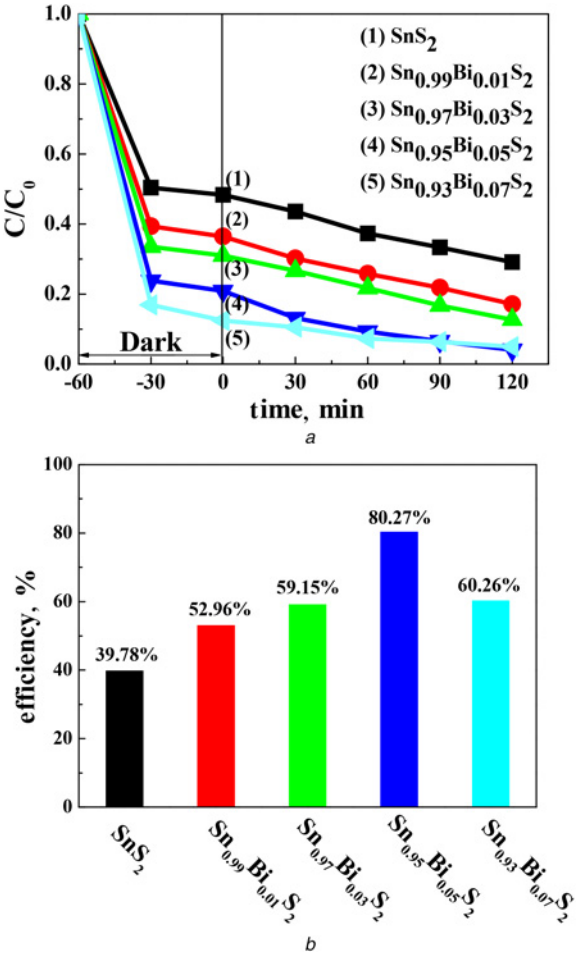

Fig. 4 *Time profile and photocatalytic efficiency of the samples*
a Time profile of C/C_0 of RhB
b Photocatalytic efficiency of the samples under the visible light irradiation

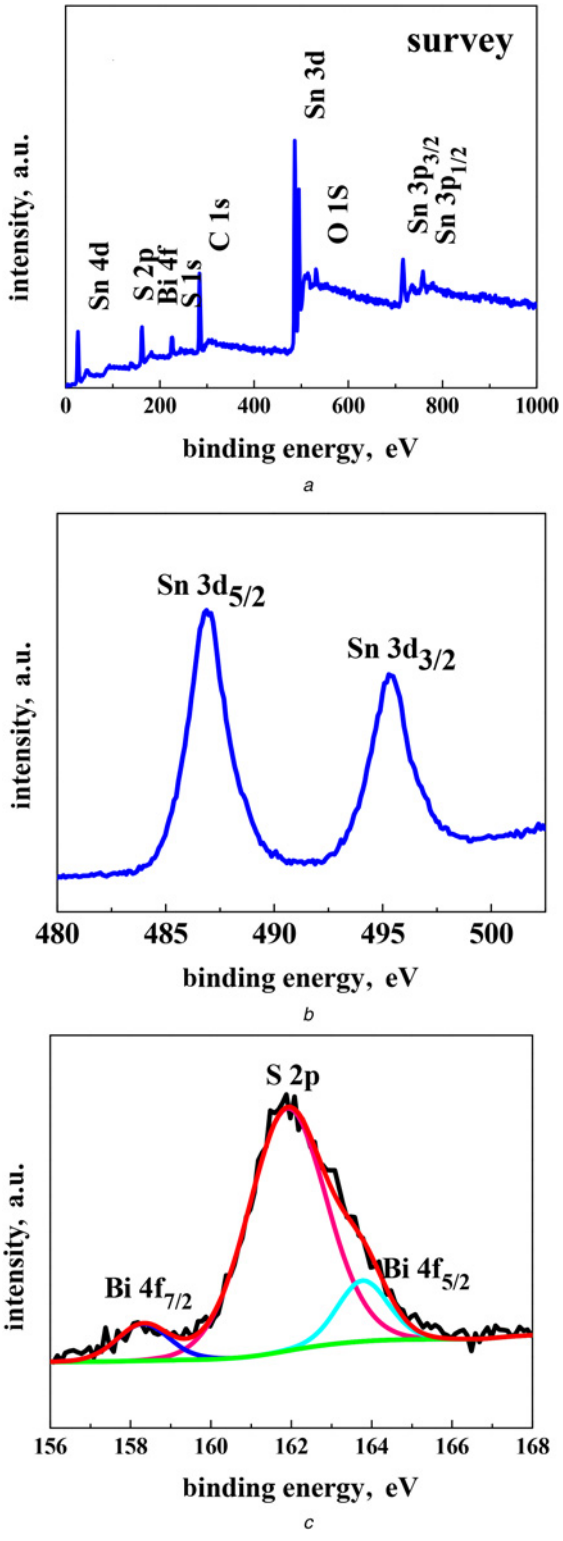

Fig. 5 *XPS spectra of*
a Survey spectra
b Sn 3d
c Bi 4f and S 2p for the as-prepared $Sn_{0.95}Bi_{0.05}S_2$

binding energies, respectively. It also indicated that Sn was 4+ state [11]. Fig. 5*c* shows the X-ray photoelectron spectroscopy (XPS) spectra of S 2p and Bi 4f. The strong peak at 161.9 eV, attributed to S 2p binding energy, was assigned to S^{2-}. Two weak peaks at 158.3 and 163.8 eV correspond to the binding energies of Bi $4f_{7/2}$ and Bi $4f_{5/2}$, respectively, indicating Bi was 3+ state [12]. This result demonstrated the formation of Bi^{3+} and was in line with the result of XRD.

Transmission electron microscopy (TEM) is usually adopted to observe the morphology of the as-prepared products [13]. In Fig. 6*a*, it can be seen that most pure SnS_2 particles were hexagonal nanosheets with the size of 30–50 nm, as is shown as the white arrows. Moreover, in Fig. 6*b*, it shows that the as-prepared $Sn_{0.95}Bi_{0.05}S_2$ had similar morphology with pure SnS_2. This result indicated that doping Bi^{3+} could not obviously change the morphology of pure SnS_2. Fig. 6*c* shows the high-resolution TEM (HRTEM) image of the as-prepared $Sn_{0.95}Bi_{0.05}S_2$. It can be seen that the lattice fringe spacing was 0.278 nm, corresponding to the (011) plane of $Sn_{0.95}Bi_{0.05}S_2$.

Electrochemical impedance spectroscopy was employed to prove the charge transfer resistance and the separation efficiency between the photogenerated electrons and holes. EIS of pure SnS_2 and the as-prepared $Sn_{0.95}Bi_{0.05}S_2$ is shown in Fig. 7. It can be seen that the arc radius of the as-prepared $Sn_{0.95}Bi_{0.05}S_2$ was significantly smaller than that of pure SnS_2, indicating that the as-prepared $Sn_{0.95}Bi_{0.05}S_2$ possessed lower charge transfer resistance than that of pure SnS_2. This could further support that the as-prepared $Sn_{0.95}Bi_{0.05}S_2$ had more effective electron–hole pair separation and higher degradation efficiency than that of pure SnS_2.

The active species trapping experiments for degradation of RhB over the as-obtained $Sn_{0.95}Bi_{0.05}S_2$ were carried out to analyse the photocatalytic mechanism. The ethylenediamine tetraacetic acid (EDTA), benzoquinone (BQ) and t-butanol (TBA) were separately used as h^+, O_2^- and ·OH scavengers, respectively [14]. The results are shown in Fig. 8. It can be observed that after using the scavengers, the photocatalytic activity was suppressed. It is worth

© The Institution of Engineering and Technology 2017

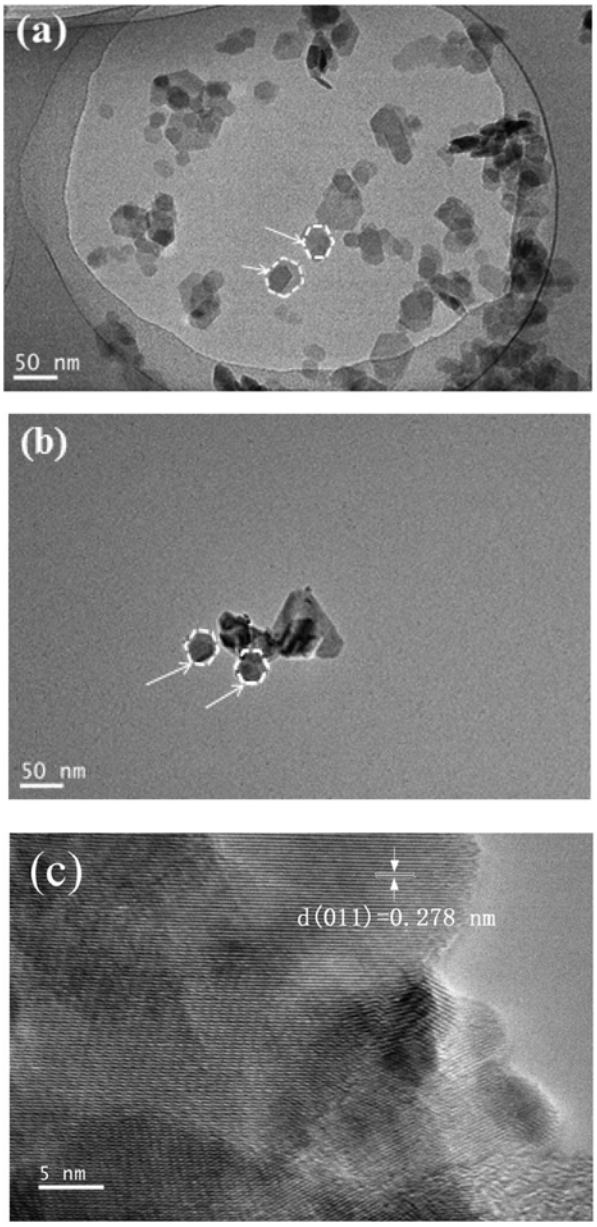

Fig. 6 *TEM images of*
a Pure SnS_2
b As-prepared $Sn_{0.95}Bi_{0.05}S_2$
c HRTEM images of the as-prepared $Sn_{0.95}Bi_{0.05}S_2$

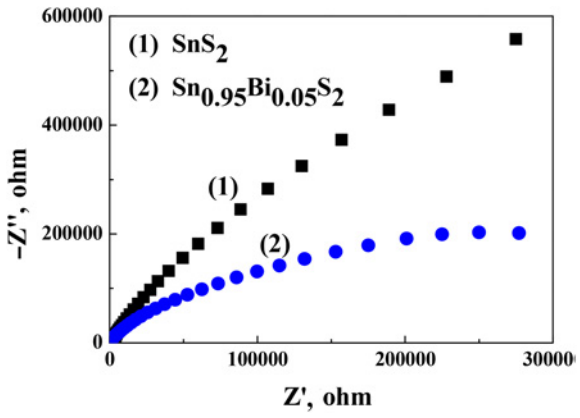

Fig. 7 *EIS Nyquist plot of pure SnS_2 and the as-prepared $Sn_{0.95}Bi_{0.05}S_2$*

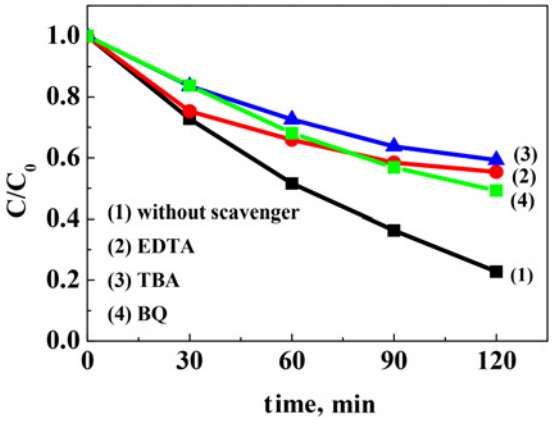

Fig. 8 *Photocatalytic degradation curves of the as-prepared $Sn_{0.95}Bi_{0.05}S_2$: (1) without using any scavenger;(2) with using EDTA; (3) with using TBA; (4) with using BQ*

noting that the scavenging effect of TBA was the most obvious, indicating that ·OH was the main active species and played the main role during the photocatalytic processes.

Based on the above results, a possible degradation mechanism of the as-prepared $Sn_{0.95}Bi_{0.05}S_2$ is proposed in Fig. 2. It can be seen that the as-prepared $Sn_{0.95}Bi_{0.05}S_2$ could be excited more easily by Xe light to produce photogenerated electrons and holes due to very narrow bandgap. Moreover, the photogenerated electrons could absorb O_2 to generate O_2^-; meanwhile, the holes oxidised H_2O or OH^- into ·OH. Finally, RhB was oxidised to degrade.

4. Conclusion: In summary, visible and near-infrared light responsed $Sn_{1-x}Bi_xS_2$with high purity had been fabricated through a hydrothermal method. Experimental results showed that the doping content of Bi^{3+} greatly influenced the degradation efficiency of as-prepared samples. It was first increased and then decreased with increasing the doping content of Bi^{3+}. When the mole fraction of doping Bi^{3+} was 5%, the as-prepared $Sn_{0.95}Bi_{0.05}S_2$nanosheets had the highest degradation efficiency of 95.9% in 120 min and the narrowest bandgap energy of 0.38 eV. Moreover, the as-prepared $Sn_{0.95}Bi_{0.05}S_2$ possessed more effective electron–hole pair separation than that of pure SnS_2. In addition, ·OH played the main role during the degradation. This work indicated that doping Bi^{3+} was one of effective methods to improve the photocatalytic degradation efficiency, narrow the bad gap energy of pure SnS_2 as well as promote its application in photocatalytic degradation of organic dye.

5. Acknowledgments: This work was funded by Natural Science Foundation of Hebei Province, China (grant no. E2013210011). The authors declare that they have no conflict of interest.

6 References

[1] Wu X.F., Li H., Sun Y., *ET AL.*: 'Synthesis of SnS_2/few layer boron nitride nanosheets composites as a novel material for visible-light-driven photocatalysis', *Appl. Phys. A, Mater.*, 2017, **123**, p. 709
[2] Wu X.F., Zhao Z.H., Sun Y., *ET AL.*: 'Few-layer boron nitride nanosheets: preparation, characterization and application in epoxy resin', *Ceram. Int.*, 2017, **43**, pp. 2274–2278
[3] Jiang Z.Y., Liu Y.Y., Jing T., *ET AL.*: 'Enhancing visible light photocatalytic activity of TiO_2 using a colorless molecule (2-methoxyethanol) due to hydrogen bond effect', *Appl. Catal. B, Environ.*, 2016, **200**, pp. 230–236
[4] Sonia S., Poongodi S., Suresh Kumar S., *ET AL.*: 'Hydrothermal synthesis of highly stable CuO nanostructures for efficient photocatalytic degradation of organic dyes', *Mat. Sci. Semicon. Proc.*, 2015, **30**, pp. 585–591

© The Institution of Engineering and Technology 2017

doi: 10.1049/mnl.2017.0727

[5] Cao J., Xu B., Lin H., *ET AL.*: 'Novel heterostructured Bi_2S_3/BiOI photocatalyst: facile preparation, characterization and visible light photocatalytic performance', *Dalton T.*, 2012, **41**, pp. 11482–11490
[6] Wang J.G., Chen Y.J., Zhou W., *ET AL.*: 'Cubic quantum dot/hexagonal microsphere $ZnIn_2S_4$ heterophase junction for exceptional visible-light-driven photocatalytic H_2 evolution', *J. Mater. Chem. A*, 2017, **5**, pp. 8451–8460
[7] Qu J.F., Chen D.Y., Li N.J., *ET AL.*: 'Coral-inspired nanoscale design of porous SnS_2 for photocatalytic reduction and removal of aqueous Cr(VI)', *Appl. Catal. B, Environ.*, 2017, **207**, pp. 404–411
[8] Li H.B., Zhang J., Huang G.Y., *ET AL.*: 'Hydrothermal synthesis and enhanced photocatalytic activity of hierarchical flower-like Fe-doped $BiVO_4$', *T. Nonferr. Metal. Soc.*, 2017, **27**, pp. 868–875
[9] Zhang J., Liu S., Yu J., *ET AL.*: 'A simple cation exchange approach to Bi-doped ZnS hollow spheres with enhanced UV and visible-light photocatalytic H_2 production activity', *J. Mater. Chem.*, 2011, **21**, pp. 14655–14662
[10] Cui X., Xu W., Xie Z., *ET AL.*: 'Effect of dopant concentration on visible light driven photocatalytic activity of $Sn_{1-x}Ag_xS_2$', *Dalton T.*, 2016, **45**, pp. 16290–16297
[11] Tu J.R., Shi X.F., Lu H.W., *ET AL.*: 'Facile fabrication of SnS_2 quantum dots for photoreduction of aqueous Cr(VI)', *Mater. Lett.*, 2016, **185**, pp. 303–306
[12] Jiang Y.F., Hu J.C., Li J.L.: 'Synthesis and visible light responsed photocatalytic activity of Sn doped Bi_2S_3 microspheres assembled by nanosheets', *RSC Adv.*, 2016, **6**, pp. 39810–39817
[13] Wu X.F., Li H., Sun Y., *ET AL.*: 'One-step hydrothermal synthesis of $In_{2.77}S_4$ nanosheets with efficient photocatalytic activity under visible light', *Appl. Phys. A, Mater.*, 2017, **123**, p. 426
[14] Wu X.F., Zhao Z.H., Sun Y., *ET AL.*: 'Preparation and characterization of Ag_2CrO_4/few layer boron nitride hybrids for visible-light-driven photocatalysis', *J. Nanopart. Res.*, 2017, **19**, p. 193

© The Institution of Engineering and Technology 2017